

Hamiltonian Cycles on Symmetrical Graphs

Carlo H. Séquin

Computer Science Division, EECS Department
University of California, Berkeley, CA 94720
E-mail: sequin@cs.berkeley.edu

Abstract

The edges of highly-connected symmetrical graphs are colored so that they form Hamiltonian cycles. As an introduction we discuss the coloring of the complete graphs K_{2m+1} for $m > 1$, but the focus is on the graphs resulting from symmetrical perspective projections of the edges of the regular 4-dimensional polytopes into 3-space. The goal is to color all edges in these graphs with multiple congruent copies of Hamiltonian cycles exhibiting as much symmetry as possible.

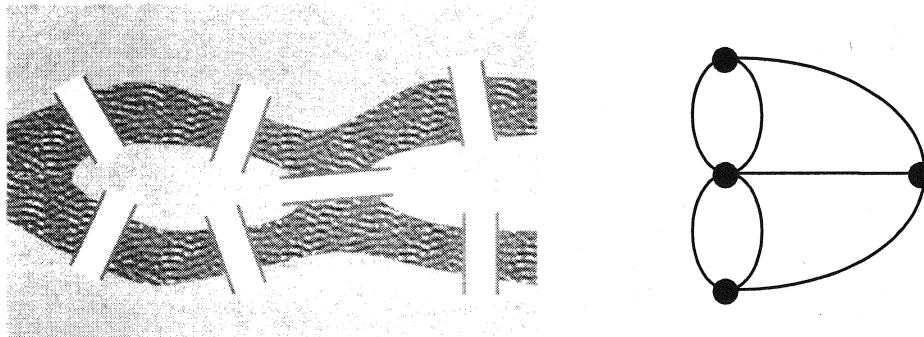


Figure 1: Map of Königsberg (a) and equivalent graph (b).

1. Introduction

In 1735, Euler learned of a popular problem in the town of Königsberg: Is it possible to cross all seven bridges in this town exactly once and then return to the starting point? This can be seen as a graph problem. With a suitable degree of abstraction, the city map can be reduced to a graph (Fig. 1) with just seven edges, i.e., the seven bridges, and with just four nodes representing the quarters in town from which these bridges emerge. Euler quickly showed that the desired tour was not possible, and as a generalization of the Königsberg bridge problem, also showed (without proof) that a connected graph has an Eulerian circuit iff it has no vertices of odd valence. In this context, let's review the following definitions:

- **Euler Path:** A path on a graph whose edges consist of all graph edges.
- **Eulerian Circuit (or Cycle):** An Eulerian path that starts and ends at the same vertex.
— In other words, it is a graph cycle that uses each edge exactly once.
- **Hamiltonian Path:** A path on a graph that visits each vertex exactly once.
- **Hamiltonian Circuit (or Cycle):** A Hamiltonian path that is simultaneously a graph cycle.

The general goal is to cover a graph completely by using several Hamiltonian cycles. If this can be achieved, then the individual cycles can readily be stitched together at vertices through which more than one cycle passes, and this combination would then readily yield also an Eulerian Circuit.

However, we are specifically interested in the coloring of graphs of high symmetry while maintaining as much of that symmetry as possible in our edge coloring. Specifically we will look at the 6 graphs that result from symmetrical perspective projections of the edges of the six regular 4-dimensional polytopes into 3-space. The simplest ones can be done with just two colors; but the regular 600-Cell with 120 vertices and 720 edges needs six colors, since each one of its vertices is of valence 12. In all cases, we would like to find colorings that consist of mutually congruent Hamiltonian cycles – no matter how many are involved.

To set the stage, let's briefly look at a couple of examples of edge graphs resulting from 3D regular solids. For instance, can we find a solution of the desired type of path for the cube? We can readily see that an Eulerian cycle cannot exist, since not all valences are even. Neither can we find an Eulerian path, since there are more than two vertices of odd valence. On the other hand, we can readily find a Hamiltonian cycle (Fig.2a). But we cannot complete the coloring of this graph with a second Hamiltonian cycle, since there are only four uncolored edges left. From this example we can readily infer, that our desired solutions also requires that all the vertices in the graph are of even valence.

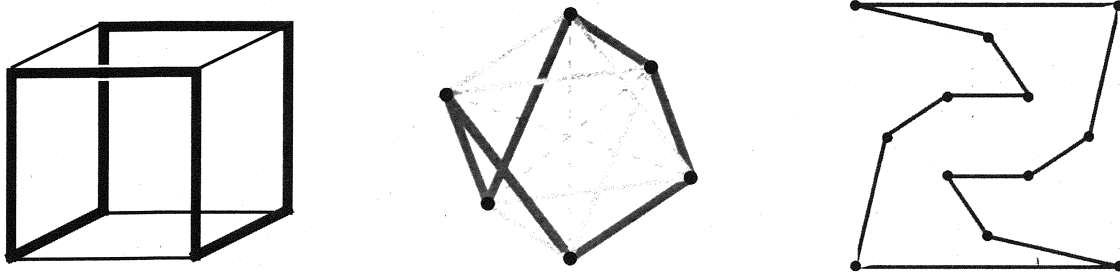


Figure 2: Hamiltonian cycles on the cube (a), the octahedron (b), and the cuboctahedron (c).

Among the Platonic solids, the octahedron is the only one whose edge graph meets this criterion. And indeed, it is possible to cover all 12 edges with two disjoint Hamiltonian cycles. With a little bit of experimentation we can even make these two cycles to be congruent (Fig.2b). On the cuboctahedron we can also find two complementary congruent cycles that individually show C_2 symmetry (Fig.2c).

2. Complete Graphs

Now let's step up to larger challenges! But let's only consider graphs with all even vertices, and let's focus on highly symmetrical graphs. First we demand topological symmetry, i.e. all vertices should have the same valence and also should have the same connectivity to other vertices. A first source of such graphs are the fully connected graphs of n nodes, K_n , in which obviously all vertices are topologically identical. However, we need to limit ourselves to odd n , so that all the nodes have even valence.

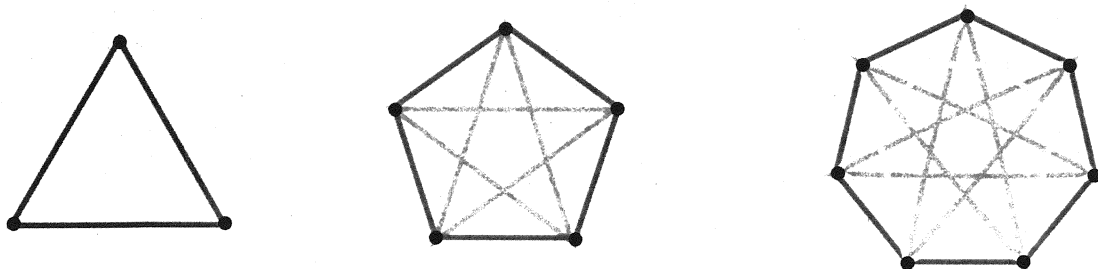


Figure 3: K_3 , K_5 , and K_7 , and their coverage with Hamiltonian cycles (a,b,c).

To obtain graphs that also have a high degree of geometrical symmetry, we arrange these nodes regularly on a circle in the plane so that the convex hull of the arrangement is a regular n -gon. K_3 has a trivial solution (Fig.3a). K_5 and K_7 readily offer nice solutions that preserves the 5-fold symmetry (Fig.3b) and 7-fold symmetry (Fig.3c), respectively; however, the different paths are not congruent.

To obtain the desired congruent paths, we need to start with a different arrangement of the vertices in the plane. We only put $n-1$ vertices onto a circle to form a regular polygon and then put the last node into the center of the circle. We note, that in the graph with $2m+1$ nodes, the valences of the vertices is $2m$, and thus we will need a total of m Hamiltonian cycles, and each cycle must pass through each vertex. Since the outer polygon has $2m$ sides, it follows that in a symmetrical arrangement every path would color two of these edges – for instance the two opposite ones, so that we obtain an almost- C_2 symmetry for each path. The inner edges in this graph come in a variety of different lengths, but for each type there are $2m$ copies, except for the maximal diagonals that directly connect opposite vertices, for which there are only m copies. With this, a simple and regular pattern emerges for coloring a subset of these edges so as to form a Hamiltonian cycle: We form a zigzag path and then connect the ends of this path with one of the maximal diagonals (Fig.4d). The superposition of m such paths, properly rotated by an angle of $180/m$ degrees, will achieve the desired symmetrical coloring (Fig.4a-c).

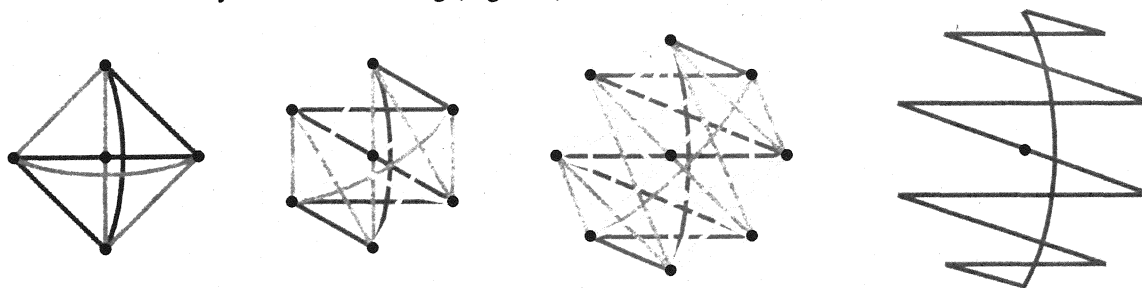


Figure 4: K_5 , K_7 , K_9 , covered with congruent Hamiltonian cycles (a,b,c), and one cycle of K_{11} (d).

3. The Simple Regular 4D Polytopes

In four dimensions there exist six regular polytopes [1]. Table 1 summarizes some of their salient geometric features and lists the valence v of the vertices, the number w of faces (or cells) sharing each edge, the number n of sides on each face, and the type of cell that makes up the shell of each polytope. Many different symmetric edge projections from 4D to a 3D subspace have been discussed and illustrated in [2]. We will focus on close-up perspective cell-first projections, where the whole 3D image is completely contained within a single outer cell. These projections maintain a high degree of symmetry and have no coinciding vertices or edges.

Table 1: Characteristics of the Regular Polytopes in 4D

	Simplex	Tesseract	16-Cell	24-Cell	120-Cell	600-Cell
# Vertices	5 ($v=4$)	16 ($v=4$)	8 ($v=6$)	24 ($v=8$)	600 ($v=4$)	120 ($v=12$)
# Edges	10 ($w=3$)	32 ($w=3$)	24 ($w=4$)	96 ($w=3$)	1200 ($w=3$)	720 ($w=5$)
# Faces	10 ($n=3$)	24 ($n=4$)	32 ($n=3$)	96 ($n=3$)	720 ($n=5$)	1200 ($n=3$)
# Cells	5 (tetra)	8 (cube)	16 (tetra)	24 (octa)	120 (dodeca)	600 (tetra)

We now try to find congruent Hamiltonian cycles that will fully color the edge graphs of these six polytopes. We start with the three least complex ones, where the solutions can readily be found by trial and error. The 4D simplex can be covered by two identical Hamiltonian cycles that nicely complement each other (Fig.5a). The 4D cross polytope (16-Cell), however, requires three colors, since all vertices are of valence 6. A very attractive symmetrical arrangement of three congruent paths has been found (Fig.5b).

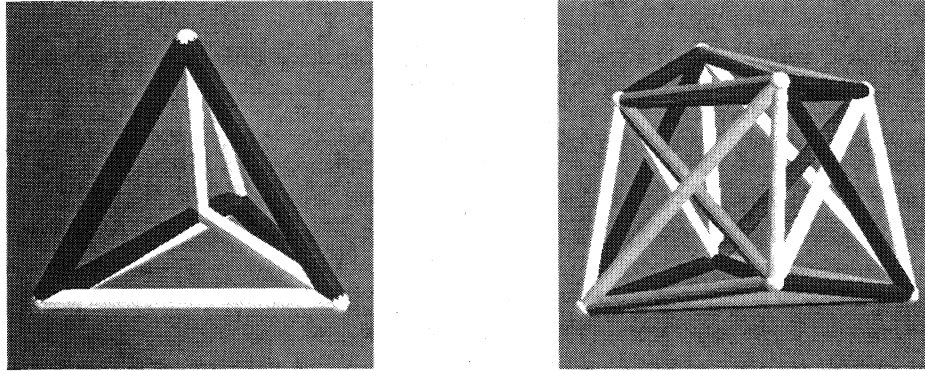


Figure 5: *Hamiltonian cycles on the 4D simplex (a) and cross polytope (b).*

The hypercube requires only two Hamiltonian cycles, since all its vertices are of valence 4. Two different valid coloring schemes – out of many possible ones – are shown in Figure 6. The second one (Fig.6b) best meets our stated goals, as it transforms one path into the other with a simple 90° -rotation around the axis perpendicular to the image plane.

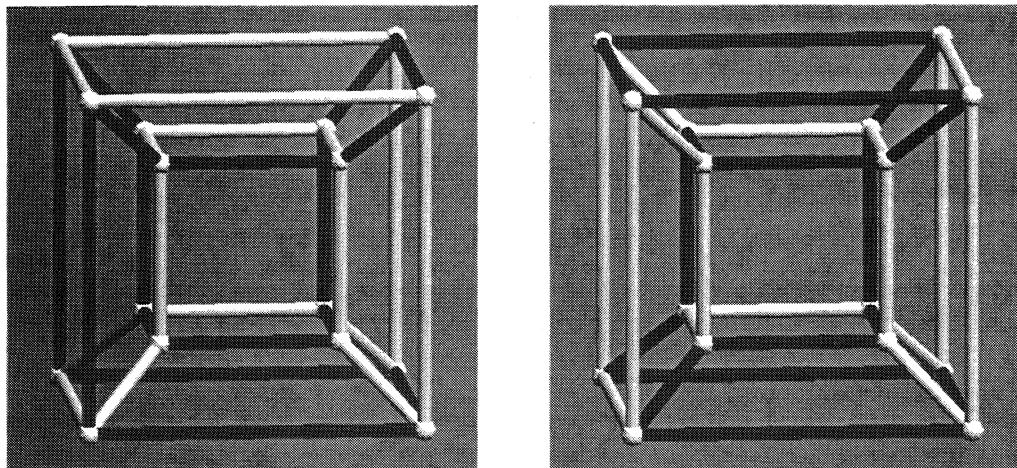


Figure 6: *Two Hamiltonian path colorings of the 4D hypercube.*

4. The 24-Cell

The 24-Cell has 24 vertices and 96 edges, and thus its graph is more challenging. Four Hamiltonian cycles are needed, since all vertices are of valence 8. Given the obvious 4-fold symmetry at each vertex, it seems natural to consider a C_4 -axis for replicating the identical Hamiltonian cycles. To make the search for a suitable solution more tractable, I used a structured approach that exploited the shell-based symmetry of this object. The cell-first projection consists of three highly symmetrical nested wire frames (octahedron, cuboctahedron, and octahedron) and two “connector sets” that link subsequent shells. If we want to obtain

an overall scheme in which the four colors transform into one another by cyclic rotations in steps of 90° around a single C_4 -axis, then that symmetry has to be reflected on each shell and also on the two connector sets. Thus I started by designing some pleasing C_4 -symmetric color arrangements for the octahedral and cuboctahedral shells. I also developed a simple interactive computer graphics visualization program that allowed me to rotate these shells individually around their common C_4 -axis, while trying to find combinations of connector edges that would connect all edges of the same color into a single Hamiltonian cycle. This approach decomposes the complex problem into a few tractable modules and moves. With the help of this program, I could find a first solution in less than two hours (Fig.7a).

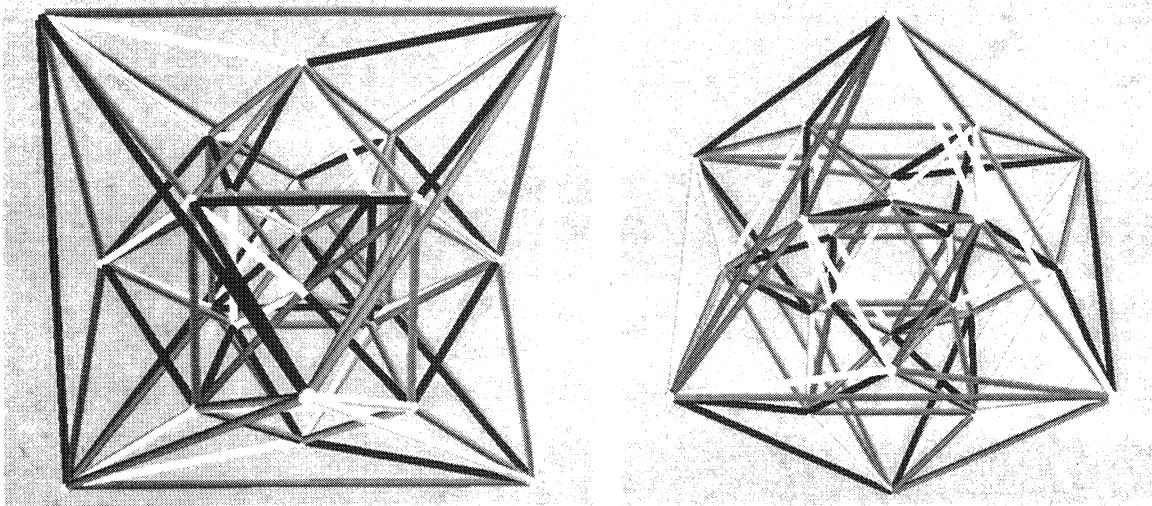


Figure 7: Four Hamiltonian cycles on the 24-Cell (a) emerging from one another by a 90-degree rotation, and (b) by moves from the tetrahedral symmetry group.

If we follow one of the Hamiltonian paths and record its progress from one shell to the next, we find the shell visitation schedule shown in Figure 8a. In this schematic, the top row of six dots represents the vertices of the outermost large octahedron. The bottom six dots correspond to innermost octahedral shell, and the twelve dots in the middle represent the intermediate cuboctahedral shell. In this schedule, each path has four sections of three consecutive edges that lie on the same shell. These sections are joined in a somewhat irregular manner. Another schedule is shown in Figure 8b. In this plan, no two edges are visited consecutively on the same shell. This schedule looks more regular and symmetrical. Can we possibly further enhance the symmetry of the colored wire frame shown in Figure 7a by switching to a different schedule?

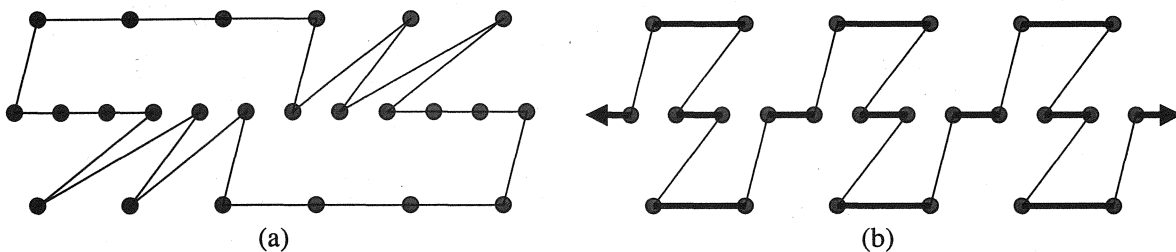


Figure 8: Two different shell-visitation schedules for the 24-Cell

The projection of the 24-Cell that we have used has not only C_4 -symmetry. It has also C_2 and C_3 symmetry axes, and overall obvious cuboctahedral and tetrahedral symmetries. Let's aim for a color arrangement with more symmetry than just one C_4 permutation axis, e.g. a tetrahedral permutation group, as

shown in Figure 9a, and more schematically in Figure 9b. The rotations around each of the four C_3 -axes, leave one color in place, while the other three are cyclically permuted for each rotation of 120° around the C_3 -axis. There are also three C_2 -axes, where a 180° rotation switches two pairs of colors simultaneously.

Clearly, each individual shell must adhere to the chosen symmetry group. Thus we first need to find suitable colorings for the octahedral and cuboctahedral shells. One solution each is shown in Figures 9a and 9c, respectively. Note that the individual shells may have some additional symmetries, that are not present in the overall constellation. For instance, the octahedral shell (Fig.9a) exhibits three C_4 -axes that cyclically permute all four colors; but such an axis is not present in the colored cuboctahedral shell. Notice also that there are no connected edges of the same color on any of these shells, in agreement with the shell visitation schedule shown in Figure 8b.

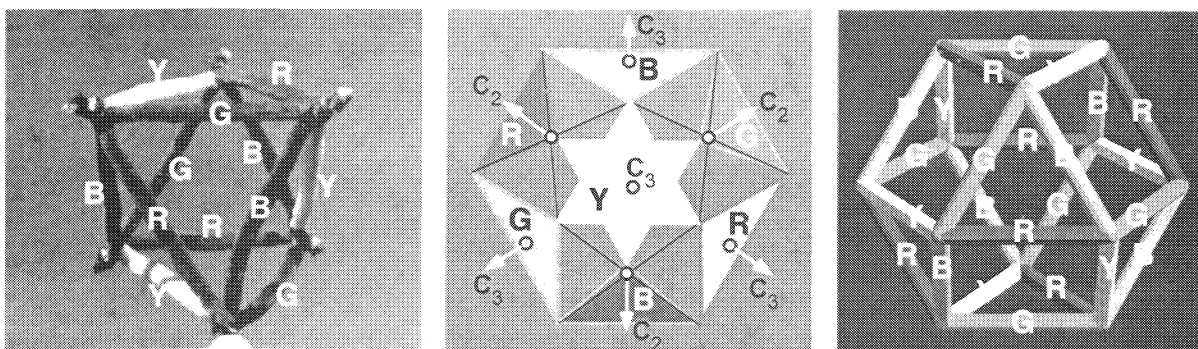


Figure 9: Tetrahedrally symmetrical coloring applied to the shells of the 24-Cell

Now we can try to complete the tetrahedral coloring for the 24-Cell by nesting the suitably pre-colored shells and subsequently trying to link them with properly colored inter-shell connector edges, so that all edges of a particular color form a single Hamiltonian cycle. It is obvious that the different shells need to be aligned in such a way that they respond in the same cyclic manner to the color permutations around any of the symmetry axes. This dramatically reduces the search space for possible constellations that may yield congruent Hamiltonian cycles. Even with this insight, it still took me many hours spread over several days to find a valid solution. The reason was that I did not realize at first that the two octahedral shells can be arranged in more than one valid orientation with respect to one another. The second possibility, which is the one used in the final solution, emerges from the first one by a point inversion through the center.

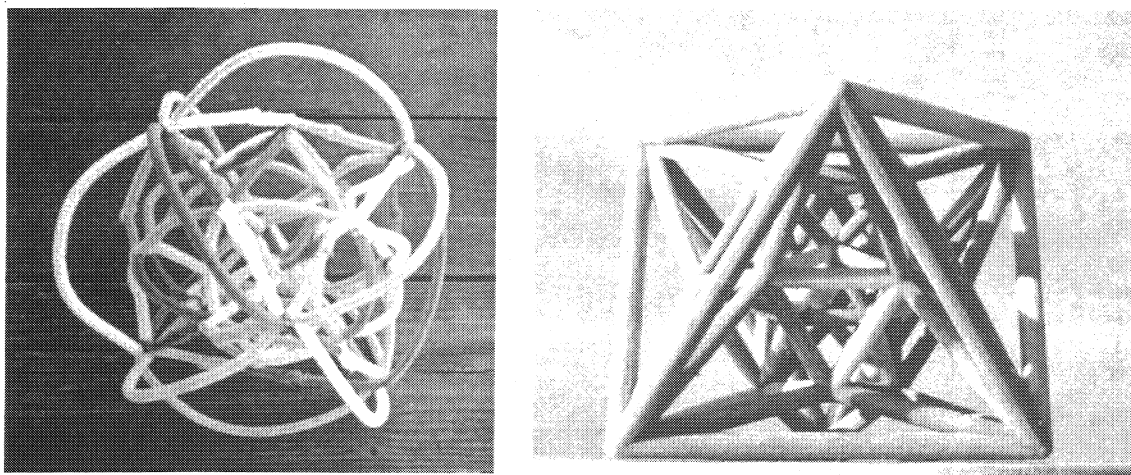


Figure 10: Physical models of the 24-Cell: Pipe-cleaner model (a), 3D-Color-Print [4] (b).

5. The 120-Cell

Before I had found the solution for the 24-Cell and devised the shell-based approach, Mike Pao, an undergraduate researcher, had joined my quest and set out to find the desired solutions on the two most complex polytopes by computer search. He first programmed a brute-force backtracking search for two congruent Hamiltonian cycles of length 600 on the perspective projection of the 120-Cell. We tried to reduce the depth of the search by looking for inherent symmetries that we might find in this path. However, we quickly convinced ourselves that these Hamiltonian cycles cannot exhibit a high degree of symmetry. Neither 3-fold nor 5-fold symmetry will be possible. To prove this, consider for instance the edges circling a pentagonal face around a potential C_5 symmetry axis. The only way to maintain 5-fold symmetry with a 2-color scheme would be to make them all the same color. However, this would form a sub-cycle of length 5 – which is not allowed.

We cannot even expect C_2 symmetry for this path! Consider the edges in the dodecahedral convex hull. Any possible C_2 -axis must go through the middle of two opposite edges. There is then exactly one pair of opposite edges that are parallel to this C_2 symmetry axis. These two edges transform into one another in a 180° rotation around the C_2 -axis; thus they must be of the same color. But this leaves no equivalent edge-pair for the congruent path, which needs to have the same C_2 -axis.

Congruence between the two Hamiltonian cycles has precedence over the symmetry of an individual path. An elegant way to obtain two congruent paths for the price of one in the projection of the 120-Cell is to simply assign opposite edges in this graph to the two different paths. Mike Pao implemented a simple search algorithm that tried to add one pair of complementary path segments at a time. This was not successful; it routinely “painted itself into a corner.” The furthest we ever got was to a length of 550 segments after a run time of many hours. This is actually not too bad, considering that finding even a single Hamiltonian cycle is known to be an NP-hard computational problem.

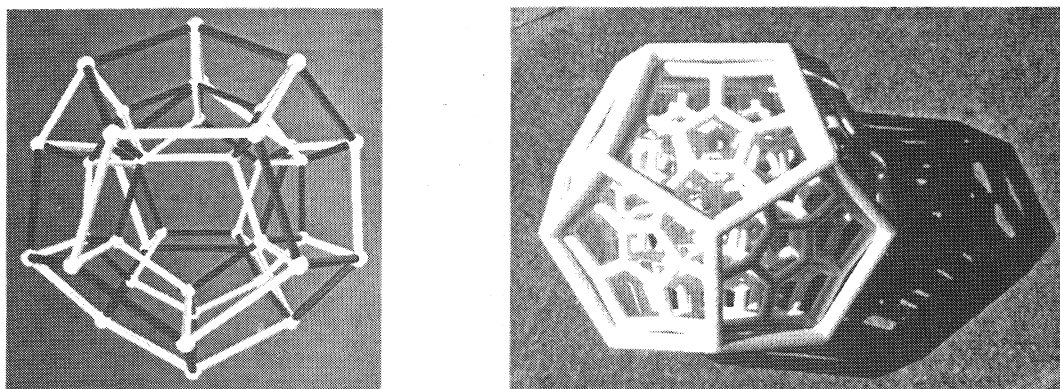


Figure 11: *Pentagonal double shell (a) compared with the full graph that needs to be colored (b).*

To clarify the issue of what symmetries can be expected for this graph, we studied a simpler problem. Two nested pentagonal shells connected with radial struts form a graph with the same symmetry and which also has all vertices of valence 4. We found a nice solution with a shell-based approach (Fig.11a). First I chose a left-right symmetrical 2-color pattern for the radial struts. Next I looked for a coloring of the outer shell that kept opposite edges at different colors, and which did not have any obvious flaws, such as merging three edges of the same color in one vertex. Then the question arose, whether a similar flawless pattern could be found for the inner shell, which at the same time would complete the path fragments on the outer shell into a single Hamiltonian cycle. It turned out that simply mirroring the pattern from the outer shell left-to-right did the trick! Now we are hopeful that a similar structured, shell-based approach will eventually yield the desired solution also for the complete 120-Cell projection (Fig.11b).

6. The 600-Cell

We also tried a basic backtracking search for the 600-Cell (Fig.12a). Here we need six different cycles, since each vertex has valence 12, but the cycles are much shorter, having only 120 segments. To reduce the danger of painting ourselves into a corner, we employed a cycle-expanding strategy. We started with a single triangle and then replaced one edge with the two other edges of an adjacent triangle, hinged to the replaced edge. Thus we always maintain a closed circuit, which can readily be expanded where there are still vertices that have not yet been touched by the Hamiltonian cycle. This strategy very quickly allowed us to find a first complete Hamiltonian cycle of length 120. Later, by enforcing a 3-fold cyclic symmetry around a chosen C_3 -axis, we also were able to construct three congruent full-length cycles concurrently.

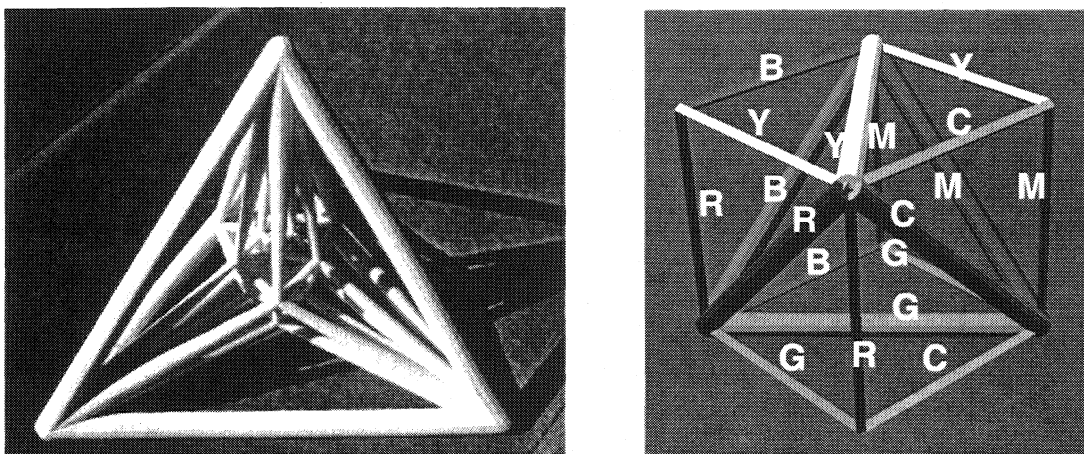


Figure 12: 3D Print of a perspective projection of the 600-Cell (a) and a possible coloring scheme (b).

But that is where the brute-force algorithm ran out of power. We were not able to add a 4th cycle to the existing three Hamiltonian cycles. We then tried to construct all six cycles in parallel while observing an overall tetrahedral symmetry for the edge coloring (Fig.12b). We also made use of the inside-outside symmetry observed in the shell schedule (Table 2) and assigned “diametrically opposite” edges (which would be opposites in the 4D original) the same color, so that our search algorithm would have to advance only through 60 moves to complete the overall task. We were able to complete up to 54 out of 60 moves, using some limited manual control over the path building process. At this point we decided to employ the more structured approach based on individually colored shells that had led to success for the 24-Cell.

7. The Shell-Based Approach

From the insights gained with the 24-Cell, a strategy emerged that should allow us to find the desired colorings of the edge graphs also for the two “monster” polytopes – the 120-Cell and the 600-Cell. We analyze the perspective projections of these polytopes by sorting all vertices into shells according to their distances from the origin. We also sort all edges into either intra-shell edges (connecting vertices of the same shell), or inter-shell edges (connecting two different shells). All these individual subsets of edges can now be analyzed separately as to the possible coloring patterns that are compatible with the chosen overall color symmetry. Now we only have to choose options from this rather limited set of possible shell colorings and check the combinations of such colorings for the formation of the desired Hamiltonian cycle. This reduces the size of the search domain substantially.

For the 600-Cell, we find that there are 15 discrete shells. Eight of them have intra-shell edges. But they are relatively sparse; no shell has more than 12 edges. Table 2 shows the complete connectivity within

and between shells that will be covered by a one of the six Hamiltonian cycles. Notice that all of the specific connector sets between any two shells are also rather sparse; at most we have to select 4 out of 24 edges for our sought-after prototype path.

Table 2: Shell and Connector Schedule for the 600-Cell

	<i>s0</i>	<i>s1</i>	<i>s2</i>	<i>s3</i>	<i>s4</i>	<i>s5</i>	<i>s6</i>	<i>s7</i>	<i>s8</i>	<i>s9</i>	<i>s10</i>	<i>s11</i>	<i>s12</i>	<i>s13</i>	<i>s14</i>
<i>s0</i>	1														
<i>s1</i>	2	0													
<i>s2</i>	2	2	0												
<i>s3</i>	2	2	4	2											
<i>s4</i>		2	2	4	2										
<i>s5</i>			2	4	4	1									
<i>s6</i>				2	0	2	0								
<i>s7</i>				2	4	4	2	0							
<i>s8</i>					2	0	0	2	0						
<i>s9</i>					2	4	0	4	2	1					
<i>s10</i>						2	2	4	0	4	2				
<i>s11</i>								2	2	4	4	2			
<i>s12</i>										2	2	4	0		
<i>s13</i>											2	2	2	0	
<i>s14</i>												2	2	2	1

To maintain congruence among the six Hamiltonian cycles, we set up five transformations that copy the prototype path into its five differently colored siblings. It took us several weeks to realize that these five transformations (together with the identity) need not form a group, and that indeed for our particular graph, they cannot do so. The transformations we chose finally first flip the prototype path around the y-axis by 180° (Fig.13a). Then we rotate this pair twice through 120° around the {1 1 1}-axis (Fig.13b).

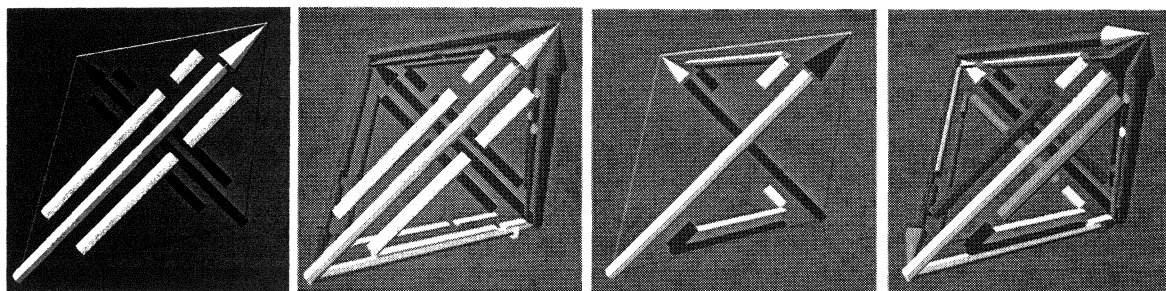


Figure 13: Symmetry transformations for coloring the 600-Cell projection (a,b,c,d).

Given that we have to accommodate six different colors in the same permutation pattern in every one of the above rather sparse edge collections, we expect only a limited number of possible constellations for each shell or connector set. For shells *s0*, *s5*, *s9*, and *s14*, where we have only 6 edges each, the color pattern must correspond to a tetrahedron with six differently colored edges. (Note that this is a different tetrahedral color permutation from the one shown in Figure 9a). For the new transformation pattern, there are only four places on the tetrahedral frame where that prototype edge can be placed so that it will be transformed into a full coverage of all tetrahedron edges. (Edges crossing the y-axis will map onto themselves).

The shells with 12 edges have a typical configuration that corresponds to an “exploded” tetrahedron with four separated faces. We can choose the placement of a first prototype edge freely (Fig. 13c), and the second one with some constraints so as not to interfere with the siblings of the first one. The most complex shells with 24 edges (Fig.13d) decompose into two half-shells with 12 edges. Notice, that Table 2 also shows an inside-outside symmetry. We believe that the color-assignment work can be cut in half if we apply the same coloring pattern (after also applying a point inversion at the center) to sibling shells whose index labels add up to 14. This same inside-outside symmetry pattern is also observed on the 24-Cell (Fig.10b) and in the pentagonal double shell (Fig.11a).

With the 600-Cell, we went through several false starts with the type of symmetry that we built into our search, and we only gained clarification of these issues after we had constructed a simpler “placeholder” problem that reflected some of the salient features of the graph that we try to color. As for the case of the 120-Cell, we were looking for a simpler graph with fewer shells but with the same inherent symmetries. But this time, even constructing the reduced graph was a rather challenging task. First, all its vertices need to be of valence 12; we like it to be of high symmetry; and we like to avoid edge intersections. The last two criteria directly contradict each other. Drawing on ideas from Section 2, we thought of using the complete graph K_{13} implemented as a dodecahedral set of points, augmented with one node at the center. However, this graph is full of edge intersections, and it does not resemble well enough the tetrahedral shape of our real problem graph. After much searching, we found a nested assembly of two tetrahedral shells and two icosahedral shells, with a total of 192 edges, to give us the desired object with the proper graph properties (Fig.14). First we convinced ourselves that the icosahedral shells could be colored with the same permutation pattern shown in Figure 13. Actually, for this pattern, the icosahedral shells of 30 edges can be decomposed into three sub-shells with not more than 12 edges, which can be colored independently. We created a computer graphics utility that allowed us to permute the colorings of these sub-shells interactively by manipulating some sliders (Fig.14b). With the help of this interactive utility, it took me typically about 5 to 10 minutes to construct a new “legal” color assignment for all the shells and their mutual connectors, so that at every vertex exactly two edges of each color join. In an hour of experimentation I found several colorings in which the edges of one color formed two, three, or four cycles. Finally I found one solution where the desired single cycle was formed – at which point I happily stopped my search. The insights gained in this exercise will be directly applicable to solving the puzzle of the projection of the 600-Cell.

8. Symmetry Considerations

The shell-based approach dramatically reduces the depth of the search tree when trying to compose a Hamiltonian cycle. The approach is based on an a priori assumption that the a set of congruent cycles actually exists. We can further reduce the search space by “building-in” some additional assumptions about the symmetries that might be exhibited by each individual path. It is a daring leap of faith to assume that such solutions with a high degree of overall symmetry actually exists, and if it works, the pay-off will be substantial. If our algorithm fails to find a solution, then we will need to relax some of our “constraints” and work through a correspondingly larger search space.

Any constraints regarding desired symmetries must be chosen very cautiously, because it is so easy to ask for something impossible. Our first trials with the 600-Cell were clearly misguided. The overall tetrahedral shape readily led us to trying to find a fully tetrahedral solution. However, the group of the oriented tetrahedron has 12 members, while we only need 6 copies of our Hamiltonian cycle. This then suggested that we might try to use the three C_2 -axes that are part of the tetrahedral group to build in some C_2 symmetry into each path itself. This may indeed lead to symmetrical colorings of the graph, but the Hamiltonian cycle will then disassociate into several smaller loops, if the path crosses the C_2 symmetry axis more than twice; and it **must** cross the axis for every vertex that lies on it!

The cycle on the 4D-Simplex (Fig.5a) can be represented with an undulating sweep suitably deformed so it forms an intriguing link (Fig.15b). The topology of the three Hamiltonian cycles on the cross polytope poses a greater challenge, since now three ribbons pass through each vertex. Rather than forming a complicated link at each node, I chose to bond the three ribbons together with a little sphere (Fig.15c). In all these sculptures, I wanted to make the continuation of each path obvious from its geometry alone, regardless of the applied coloring.

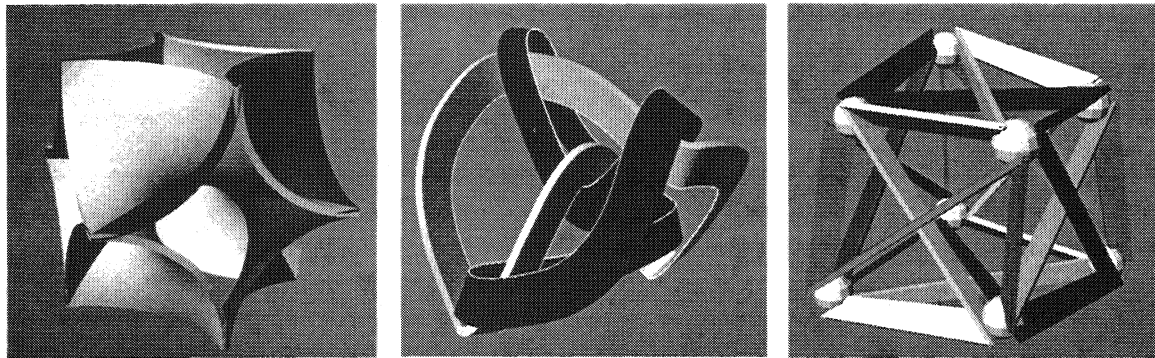


Figure 15: Sculptures derived from: Cuboctahedron (a), 4D-Simplex (b), 4D Cross Polytope (c).

10. Conclusions

One of our goals was to find mutually congruent symmetrical cycles for all six regular 4D polytopes. On the two large ones we have not yet reached our target. It is interesting to note that all the solutions presented in this paper have been found manually, and that the more brute-force computer searches have not yet been successful. This demonstrates that understanding the structure of these large problems is crucial and that taking symmetry into consideration in an aggressive manner can make a huge contribution. The shell-by-shell approach to coloring looks promising, and in combination with some computer-assisted search and verification, we expect it to yield complete solutions for the two “monster polytopes”. Our intuition, honed on the simpler four regular 4D polytopes, and in particular our solutions of the 24-Cell and our studies of the partial shell assemblies with the symmetries of the two large projections, tell us that there is a high probability that interesting “congruent” cycles can also be found for the remaining two cases – even though their full symmetry may only be apparent in 4-dimensional space.

Acknowledgements

Thanks to Euzane (Mike) Pao for the programming efforts on the 600-Cell and 120-Cell graphs and to George W. Hart for his comments on the manuscript. This work was supported through MICRO research 03-077, “Collaborative Design Environment” and by the CITRIS Institute, one of the California Institutes for Science and Innovation (CISI).

References

- [1] H. S. M. Coxeter, *Regular Polytopes*. McMillan Co. N.Y. (1963).
- [2] C. H. Séquin, *3D Visualization Models of the Regular Polytopes in Four and Higher Dimensions*. BRIDGES Conference Proceedings, pp 37-48, Baltimore July 27-29, 2002.
- [3] C. H. Séquin, *Volution's Evolution*. Meeting Alhambra, ISAMA/BRIDGES Conference Proceedings, pp 13-24, Granada, July 23-25, 2003.
- [4] Z-Corporation, 3D-Printer. – <http://www.zcorp.com/>